Investigation of the hydraulic regime of a desiccated slope under both natural and simulated environmental conditions

Emma McConnell[1*], *Jessica* Holmes[1], *Ross* Stirling[1], *Colin T* Davie[1], and *Stephanie* Glendinning[1]

[1]School of Engineering, Newcastle University, Newcastle upon Tyne, UK

Abstract. Deterioration within desiccated, clay infrastructure embankments can originate from two processes: (A) preferential flow through cracks allowing deeper and faster propagation of wetting fronts, and (B) microstructural degradation, reducing soil water retention capacity. These processes are interrelated, and together act to increase surface layer exposure to intense mechanical weathering and therefore, risk of asset failure. Desiccation induced deterioration is set to intensify under future climate change projections, heightening the need to understand how these processes develop within, and deteriorate, embankment fill over time. To address this, long-term hydrological and desiccation crack monitoring of a large-scale slope, constructed within an outdoor lysimeter, has been carried out under both natural, and simulated, climatic conditions. Initial findings illustrate a highly desiccated slope has the capacity to accept a large volume of storm rainfall prior to crack closure. This volume is set to increase due to the progressive aggregation and reduction in SWR behaviour observed within the slope. The importance of antecedent conditions, both in terms of crack geometry and initial degree of saturation, at the onset of rainfall, additionally proved important as it controls the depth and magnitude of VWC change in the slope. Continued monitoring of the slope will aid our understanding of the temporal evolution of these deterioration processes.

1 Introduction

Compacted clay soils, commonly used in embankment construction, are highly susceptible to volumetric shrinkage and swelling in response to cyclic periods of drying and wetting [1]. Volumetric shrinkage causes tensile stresses between clay particles to accumulate, which will then form desiccation cracks once the overall soil tensile strength is exceeded. Desiccation cracks increase the vulnerability of clay infrastructure embankments to deterioration through exposing a greater depth of soil to more rigorous mechanical weathering. With time, a 2-3 m weathered zone of reduced strength can develop in the slope with a higher risk of failure [2]. Therefore, understanding the processes contributing to desiccation induced deterioration is crucial for early detection of instability, and therefore to ensure maintenance of key transport networks.

There are two main deterioration processes directly associated with the formation, and prevalence, of desiccation cracks: (A) increased soil permeability, and (B) microstructural degradation. Both processes initiate deterioration by altering the hydraulic behaviour of the clay. Process (A) gives the inherently impermeable clay a higher infiltration capacity, thereby increasing the amplitude and propagation depth of cyclic variations in pore water pressure, and effective stress. This process can therefore generate zones of progressively weakened clay in the crack vicinity. For Process (B), microcrack formation, weakening of particle bonds and soil aggregation combine to form a coarser, more connected micro-pore network. This reduces a clay's ability to generate, and sustain, suction during subsequent drying cycles of similar magnitude [3]. Consequently, progressive decline in soil water retention (SWR) behaviour, and suction contribution to shear strength, will be recorded with time. These two processes are interrelated, with SWR controlling the movement of water through the soil, and therefore, will determine the volume, storage, and infiltration pathways of rainwater entering a desiccated slope. As crack formation evolves temporally with climate, the hydrology of desiccated slopes is highly variable, and difficult to quantify. Improved characterisation of hydrological processes in desiccated slopes is required to better understand how these deterioration processes are established, and mature, with time.

The acceleration of deterioration in response to climate change is a further concern for already stressed infrastructure assets. Projections of hotter, drier summers will increase crack severity. Coupling this with more frequent, high intensity rainfall events in summer will increase embankment vulnerability to failure [4]. Warming, and more prolonged periods of wetting, in winter will amplify the extremity of swelling and dry-wet cycle transitions. Available records highlight a strong correlation between peak rainfall and embankment failures, which usually follow prolonged winter wetting and intense rainfall in summer [2]. Therefore, understanding the deterioration due to cracking under current environmental conditions, and future climate extremities, is crucial to understand the deterioration of

* Corresponding author: e.l.mcconnell2@newcastle.ac.uk

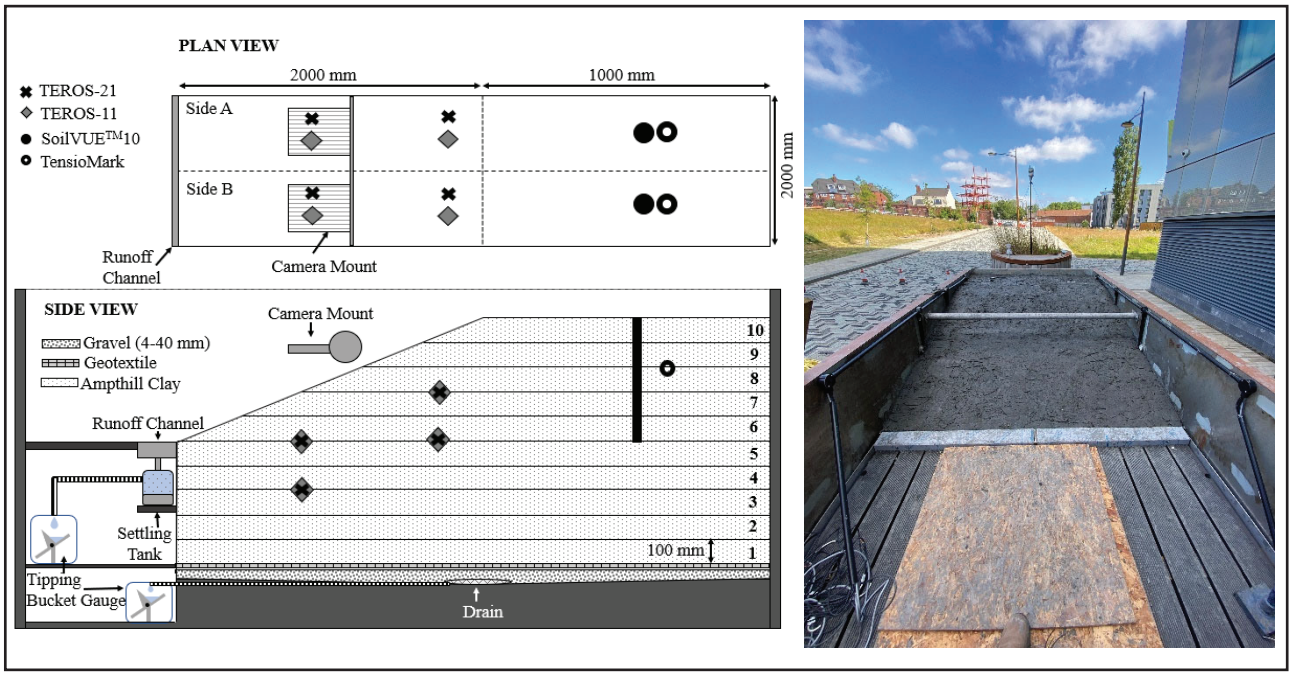

Fig. 1. Plan and side view of the slope constructed within the outdoor lysimeter. Sensor installation and monitoring equipment are marked on the diagram (left). Photograph of lysimeter slope (right).

desiccated embankments through time.

There are a limited number of studies available in the literature that investigate deterioration in slope hydrology due to desiccation at: (1) scales and compositions comparable to live infrastructure embankments; (2) under environmental conditions representative of both current, and projected, weather patterns; (3) over timescales that are realistic for deterioration to be measurable. This study has been designed to provide real-time, and long-term, hydrological and desiccation crack monitoring of a large-scale slope, constructed within an outdoor lysimeter. The slope has been subjected to both natural climatic conditions and simulated storms. This will aid our understanding of the temporal evolution of current, and future, deterioration processes that occur within desiccated infrastructure embankments.

2 Methodology

2.1 Lysimeter construction

Fig.1 illustrates a slope which was constructed within a large-scale (4500 x 2000 x 1200 mm) lysimeter located outdoors at the UKCRIC National Green Infrastructure Facility at Newcastle University, UK. The lysimeter base sloped towards a central drain to collect and measure the total drainage outflow from the soil body using tipping bucket gauges. A drainage layer – consisting of a maximum 100 mm thickness of 4 – 400 mm sized gravel – was installed at the lysimeter base. This was overlain by a layer of permeable, needle-punched, non-woven geotextile to prevent blockage of the drainage layer through washout of fines from the slope above.

The fill material used to construct the slope was the Ampthill Clay, sourced from Needingworth Quarry, near Cambridgeshire, which has been used to construct road embankments (M4 and M40) close to its source [5]. In accordance with BS 1377-2:1990 [6], the material was classified as a high to very high plasticity clay with Liquid and Plastic Limits of 71% and 27%, respectively. Following the proctor compaction method of BS1377-4:1990 [7], a maximum dry density of 1.52 Mg/m^3 was achieved at an optimal gravimetric moisture content (GMC) of 26% for the Ampthill Clay. Particle sized distribution identified the clay, silt and sand fractions of the Ampthill Clay to be 64%, 31% and 5%, respectively.

The main body of the slope was constructed from ten compacted layers of Ampthill Clay, each 100 mm thick. As demonstrated in Fig.1, the slope consisted of a flat, 1000 mm by 2000 mm slope crest with overall soil depth 1000 mm. The slope itself maintained a 1:4 geometry, tapering across 2000 mm towards a slope toe of 500 mm soil depth. No pre-processing of the Ampthill Clay was conducted prior to slope construction to reproduce the natural heterogeneity present in live assets. Following guidance on embankment construction using plastic clays, the Ampthill Clay was compacted wet of optimum to allow for most swelling to occur prior to compaction. In-situ sampling, using moisture density rings, demonstrated that the slope achieved an average dry density and GMC of 1.284 Mg/m^3 and 39%, respectively.

2.2 Sensor and monitoring installation

A cross-sectional plan of sensor installation within the slope is provided in Fig.1. The slope has been separated into Sides A and B for locality identification, however sensor installation was identical in both. In the slope crest, each side contains a water content profiler based on time-domain reflectometry (SoilVUE^{TM}10), which records volumetric water content (VWC), permittivity, electrical conductivity and temperature at 50-, 100-, 200-, 300-,

400- and 500-mm depth. At 200 mm depth, a TensioMark was installed to measure suction. Soil suction (TEROS-21) and VWC (TEROS-11) sensors were co-located at 200- and 400-mm depth in the upper and lower slope regions. The TEROS-11 also measures soil temperature and electrical conductivity.

At the slope toe, a collector channel, which drains into a tipping bucket gauge, was installed to capture runoff from the slope. Environmental monitoring of air temperature, wind speed and direction, solar radiation, relative humidity and rainfall was carried out via an on-site weather station.

Two fixed camera mounts were secured to a centrally located, structural pole covering the mid- to lower-slope region of both Sides A and B. This allowed regular photographing of a consistent frame to capture changes in crack pattern and intensity, through time and in response to changing environmental conditions. To obtain measurements of Crack Intensity Factor (CIF), defined as the ratio of cracked soil to total soil area, in addition to crack width, orientation and length, images were processed within MATLAB using a three-stage process. Firstly, pre-processing of the images was required to eliminate noise. This was carried out by adjusting image contrast and applying a Gaussian Filter to blur noise in the image. After pre-processing, binary segmentation was conducted to separate the foreground "true" pixels, representing cracks, from the background "false" pixels, containing intact clay. Adaptive thresholding was used to achieve this as it is the most effective process when dealing with uneven image illumination.

Region analysis was then performed last to analyse crack characteristics. The same pre-processing steps were applied to all images to ensure consistency in results. However, it should be noted that due to the inconsistency in outdoor lighting conditions across images, and deterioration of the soil surface through time, total noise removal was unachievable. Therefore, values within region analysis should be used as a comparative measure of crack morphology rather than absolute values.

2.3 Soil water retention determination

A laboratory soil-water retention curve (SWRC) for the Ampthill Clay was determined for the same conditions as the lysimeter slope – 39% GMC and 1.284 Mg/m^3 dry density. This was carried out by combining results from the HYPROP Simplified Evaporation Method (SEM) setup and WP4C Dewpoint PotentiaMeter to achieve both the wet and dry ends of the SWRC, respectively. The inbuilt HYPROP-FIT software was then used to fit the Fredlund-Xing [8] hydraulic function to the dataset. More information on these methods can be obtained within the manufacturer support publications.

Co-locating suction and VWC sensors at the same depth throughout the slope was to enable in-situ SWRCs to be produced. This would allow any deterioration in SWR behaviour through time to be captured. To achieve this, two major drying cycles, in which significant suction was generated, were identified. Drying Cycle 1 (DC1) was established post-construction in July 2021 and ended at the onset of an intense, natural rainfall event in September 2022. Drying Cycle 2 (DC2) initiated in April 2022 and was terminated in August 2022 at the onset of the rainfall simulations. The suction and VWC sensor data was input into the HYPROP-FIT software and the Fredlund-Xing [8] hydraulic function was fitted.

2.4 Rainfall simulations

High intensity, summer rainfall events are projected to increase in frequency with climate change. Therefore, to investigate the response of a desiccated slope under these projections and compare the results to those generated under the current natural climate, a 2 m by 2 m rainfall simulator was deployed (Fig.2). The rainfall simulator was constructed from a steel framework, which supported a pipe network that supplied 102, uniformly spaced, drip nozzles with water to produce an outflow rate of 2L/hour. This setup allowed application of three, 1 in 100 year + 45% storms, with each simulation one week apart from the 23/08/2022 until the 06/09/2022. Each storm duration was 1 hour, with 52 mm of rainfall being applied to the desiccated slope during this period. The slope was exposed to natural environmental conditions between simulations to additionally investigate the role of antecedent conditions within the slope, at the onset of storm events.

Fig. 2. Photograph illustrating the placement of the rainfall simulator on top of the lysimeter to apply storm events.

3 Results and Discussion

3.1 Changes in SWR Behaviour

Fig.3 contains the SWRCs for DC1 and DC2 within the lysimeter, in addition to the laboratory control sample. From DC1 to DC2 the air entry value (AEV), marking the onset of desaturation, reduces from approximately 50 kPa to 0.16 kPa. For DC1, saturation is maintained over a greater range of suction values compared to that of DC2 however, the maximum VWC recorded in DC2 is 20% greater than that of DC1. Additionally, the desaturation portion of the SWRC steepens between DC1 and DC2, with the maximum suction reached higher for DC1 at 180 kPa compared to 145 kPa for DC2.

The changes observed in SWR behaviour, after one year of exposure to the natural environmental conditions, suggests microstructural degradation is occurring within

the lysimeter slope. A reduction in AEV suggests development of a coarser pore network. This is indicative of desiccated soils where macro-crack development lowers the clay's ability to generate and maintain, high suctions. This coarser pore network would increase the space for water storage, supported by the higher initial VWC in DC2. Steepening of the desaturation portion of the SWRC highlights a transition to a more uniform and coarser, pore network of enhanced connectivity. This change in pore geometry and connectivity is characteristic of microstructural degradation from micro-crack formation, weakening of particle bonds and particle aggregation. These findings were also observed in the SWRCs of the full-scale BIONICS field embankment, presented within Stirling et al [3]. Further long-term monitoring of the lysimeter slope is required to determine whether continual decline in SWR and therefore microstructural degradation, occurs with time.

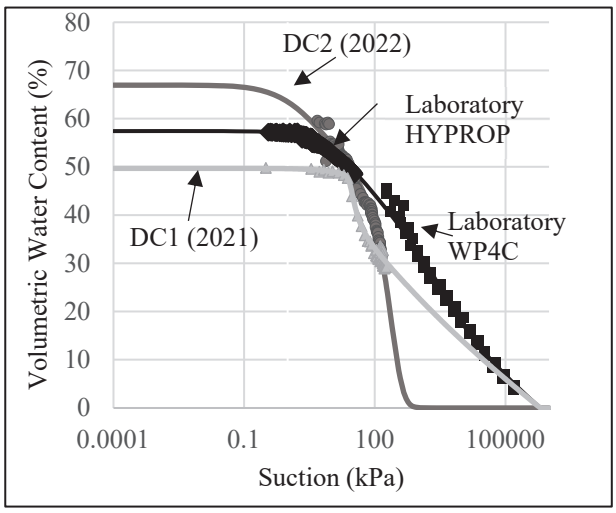

Fig. 3. SWRC for Drying Cycle 1 (DC1) occurring in Summer 2021, Drying Cycle 2 (DC2) in Summer 2022 and a laboratory SWRC composed of results from HYPROP and WP4C test methods.

3.2 Hydrology of Desiccated Slopes

Presented in Fig.4 are the changes in VWC recorded through the slope crest during the three rainfall simulations (S1 – S3) and naturally occurring rainfall events. The difference in extremity of the simulated storms compared to naturally occurring rainfall can be observed. Also presented are suction measurements at 200 mm depth within the slope crest. These are compared with daily evapotranspiration (ETo), rainfall and runoff records for the same period, in addition to crack evolution both qualitatively, with photographs (C1 – C6 in Fig.4), and quantitatively, from CIF data.

In general, saturation increases, and sensitivity to climate decreases, with slope depth. Surface layers are quickest to desaturate post rainfall as water infiltrates, under gravity, through the slope depth. Significant changes in VWC are recorded in response to the application of S1 – S3. However, the depth in which these changes are most pronounced vary between each simulation. For S1, the largest increase in VWC is recorded at 300- and 400-mm depth. This is similar for S2 however, the size of the peaks generated are reduced. Conversely, for S3, it is at 200-mm depth that the slope becomes significantly more saturated, after a muted response in S1 and S2. Shallower depths (50 – 100 mm) also increase in saturation, however in smaller steps than the deeper depths.

This variation in response depth between S1 – S3 could be attributed to the crack network present at the onset of the simulation. For S1 and S2, the CIF is high, with large primary cracks (300 – 400 mm depth) enclosing smaller secondary cracks (max. 50 mm depth), as shown in C1 and C3 within Fig.4. Preferential flow of rainwater into this crack geometry would produce the marked increase in VWC observed at 300-400 mm and 50 mm depth. During S3, this shifts to 200- and 50-mm depth as the CIF is considerably lower at the onset of the storm, with a reduced depth and number, of primary and secondary cracks (see C5 in Fig.4).

Despite the VWC response at 200 mm being muted in comparison to other depths during S1 and S2, a rapid loss of suction is recorded. Suction develops again between the rainfall simulations, however to a fraction of the value present prior to S1. The lower suction present prior to S2, with a similar CIF as S1, highlights the ability of significant cracking to develop at low suctions. This will make the clay more vulnerable to rapid suction loss and re-saturation, thereby increasing the risk of embankment failure even at low volumes of rainfall. The increase between simulations is greater between S1 and S2 than S2 and S3, which also indicates drying was more persistent during this period.

The above is evidence of the evolutionary nature of cracks with climate, which results in variation of slope infiltration capacity with time. Prior to the onset of S1 and S2, a high CIF contributes to an increased soil porosity, and therefore, permeability of an otherwise impermeable clay. As a result, the slope accepted the total volume of water applied during S1 and S2, at a much faster rate than an intact clay. The absence of runoff during this period supports this theory. Despite a much lower CIF, this holds true for S3 also however, the CIF reached zero after S3. The occurrence of a larger, natural rainfall event (N3 in Fig.4) after S3 when cracks were closed, generated the first occurrence of runoff. When considering that the intensity and depth of cracks will increase with climate change, and combining this porosity increase with the effects of microstructural degradation (discussed in Section 3.1) the result will be a deepened weathered zone of larger storage capacity, progressively more vulnerable to failure.

Formation of desiccation cracks, and generation of runoff, are both also controlled by surface saturation. This is demonstrated by the differences in VWC response between S1 – S3. The relative increase in VWC decreases with each simulation due to the slope becoming closer to saturation at the onset of each storm. This is supported by the gradual decline in suction within the slope. Therefore, saturation is important to consider when evaluating the vulnerability of a slope to failure. Surface saturation is a function of SWR behaviour, in addition to the duration

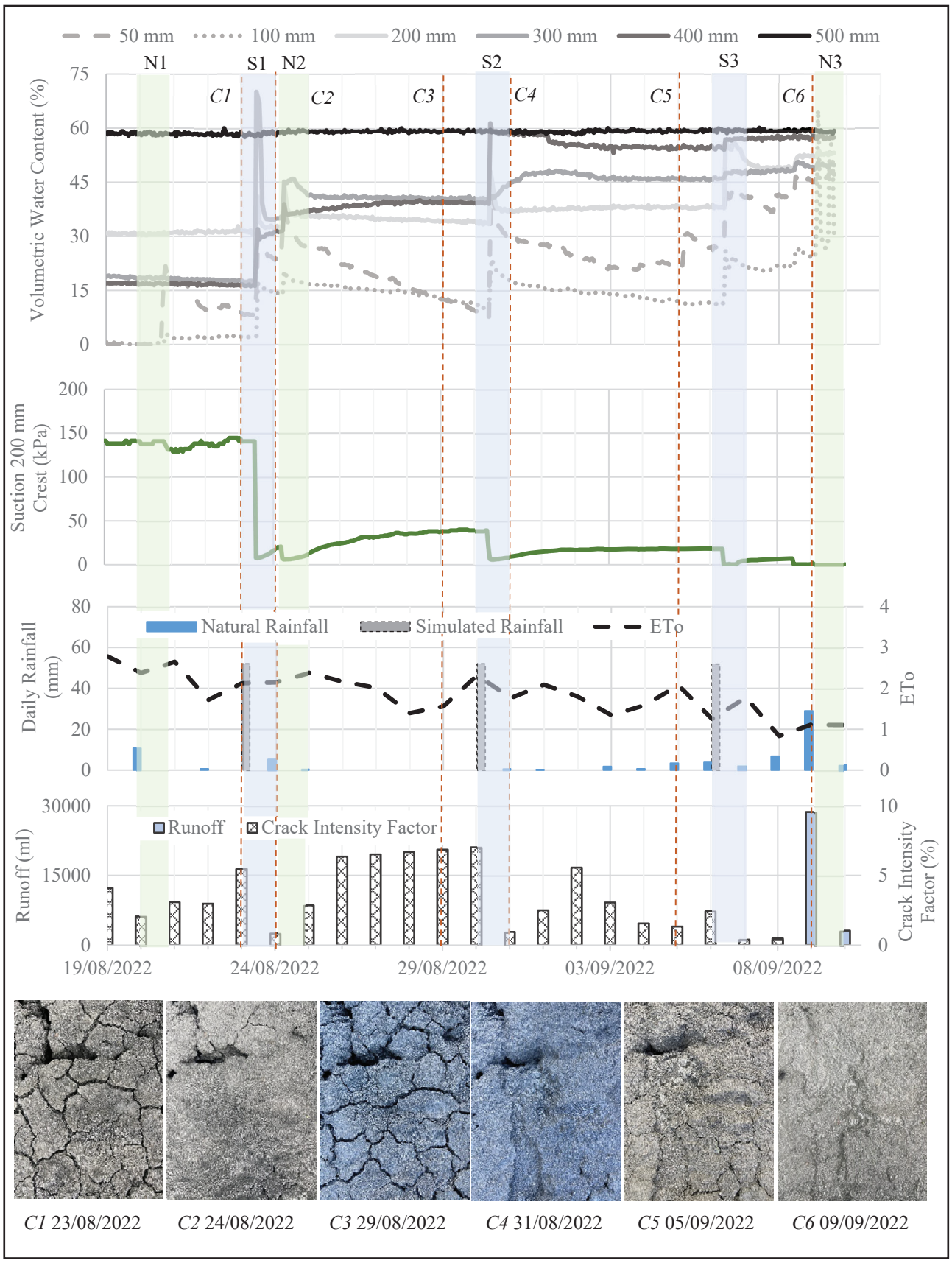

Fig. 4 Hydrological, environmental and desiccation crack time series monitoring data from 19/08/2022 until 10/09/2022 when three simulated storms were applied to the slope. Green areas highlight three natural rainfall events (N1-N3) and blue areas correspond to the three rainfall simulations (S1-S3).

and intensity of rainfall events. Prior to S1, the slope is in its driest state and suction is high. The occurrence of a natural rainfall event (N1 in Fig.4) is met with a small increase in VWC in the upper 50 mm of the slope, however suction remains high. The day after S1, a second

natural rainfall event (N2 in Fig.4) of smaller magnitude occurs however, a marked increase in VWC is recorded down to 400 mm. The difference in response between N1 and N2 can be attributed to the to the lower unsaturated hydraulic conductivity of the clay during N1 due to high suctions slowing infiltration. However, S1 -S3 were high volume, yet short duration, intense rainfall events which accelerated saturation of the slope. Runoff was generated during S1 – S3, however was captured by large primary cracks, as demonstrated in Fig.5. This accelerated the rate, and total volume, of water entering the slope via cracks. The wetting of N1 would be much lower intensity, allowing gradual wetting of the surface layers at a slower rate, preventing the formation of marked peaks in VWC. This highlights the importance of antecedent conditions in determining how a desiccated slope will respond to both seasonal norms and extreme rainfall events.

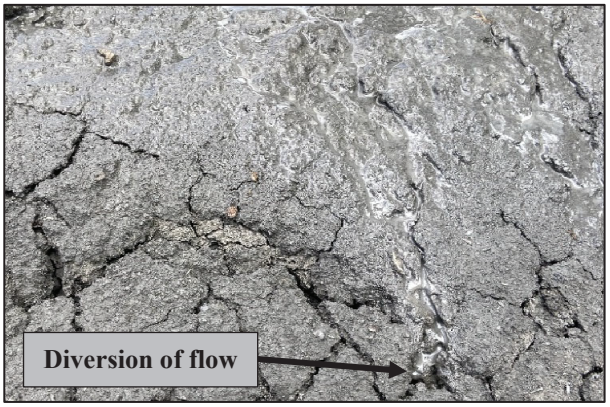

Fig. 5. Photograph illustrating the diversion of surface runoff into large primary cracks.

Fig.4 additionally demonstrates that a close sequence of mixed intensity rainfall events can accelerate saturation and therefore, runoff generation. Two days after S3, N3 (discussed previously) occurs, with VWC increase only in the upper 100 mm as the remainder of the slope had reached saturation and a large volume of runoff subsequently was generated. Runoff can accelerate deterioration of infrastructure embankments through washout of fines, evidence of which was found within the lysimeter runoff channels. With the soil becoming increasingly loose and aggregated due to micro- and macro-cracking, an additional risk of asset failure due to washout develops [2].

4 Conclusions

Initial results from long-term, hydrological and desiccation crack monitoring of a large-scale, slope constructed within an outdoor lysimeter have been presented. The experimental setup has allowed for detailed monitoring, targeted at understanding the formation and maturity of desiccation induced deterioration within infrastructure embankments.

Comparison of in-situ SWRCs from Summer 2021 and Summer 2022 demonstrated deterioration was occurring in the SWR behaviour of the Ampthill Clay. This can be attributed to a formation of a coarser, more uniform pore-size distribution which reduces soil strength by lessening suction contribution to shear strength. Further long-term monitoring is needed to see SWR deterioration progression over time.

Analysis of VWC and suction through the slope crest allowed patterns of rainfall infiltration to be observed, under different cracked states, in response to natural and simulated, rainfall events. The depth, and magnitude, of VWC change is dependent both on crack geometry, and initial degree of saturation, at the onset of rainfall. It has been demonstrated that crack patterns can recover quickly post storm events, even at low suctions, if evapotranspiration is high and rainfall is low. A series of rainfall events in close succession can be enough to close cracks and generate runoff, further putting the slope at risk from failure due to washout.

Continued long-term monitoring of the slope will be carried out to provide additional insight into the scale of desiccation induced deterioration in infrastructure embankments. Furthermore, additional simulated storm events are planned for Summer 2023. The results of these will be compared with the simulations presented in this paper to investigate changes in deterioration patterns under climate change projections.

The authors would like to thank Zelong Yu, Richard Taggart, Narryn Thaman, Daniel Green, Gareth Wear, Michael Finlay and Stuart Patterson for their help in the construction of the lysimeter. This research is funded by the UK Engineering and Physical Sciences Research Council (ESPRC) ACHILLES grant number EP/R034575/1.

References

1. M. Dyer, S. Utili & M. Zielinski. *Field survey of desiccation fissuring in flood embankments.* Water Management, 162(WM3): 221-232, (2009).
2. R. Mair, D. Hight & B. McGinnity. *A Review of Earthworks* Management, Network Rail, 543, (2021).
3. R.A. Stirling, D.G. Toll, S. Glendinning, P.R. Helm, A. Yildiz, P.N. Hughes & J.D. Asquith. *Weather-driven deterioration processes affecting the performance of embankment slopes*. Geotechnique, **71**(11), 956-969, (2020).
4. Met Office. *UKCO18 Science Overview Executive Summary*. Crown Copyright, (2019).
5. R.A. Nicholls. *M40 Oxford-Birmingham geology and geotechnics of the Waterstock-Banbury section,* in Proceedings of Institution of Civil Engineers, **104**(4), 283-295, (1994).
6. British Standard 1990. Methods of test for Soils for civil engineering purposes 1377-Part 2: Classification tests. London: British Standards Institution.
7. British Standard 1990. Methods of test for Soils for civil engineering purposes 1377-Part4: Compaction related tests. London: British Standards Institution.
8. D.G. Fredlund & A. Xing. *Equations for the soil-water characteristic curve.* Canadian Geotechnical Journal, **31**(4), 521-532, (1994).